Application of hyperspectral reflectance for early detection of dry root rot and fusarium wilt in chickpea (Cicer arietinum L.)

Vaibhav B. Thange
Vaibhav S. Malunjkar
Sunil A. Kadam
Pawan Kulwal
pawankulwal@gmail.com

Mahatma Phule Krishi Vidyapeeth https://orcid.org/0000-0002-3077-183X

Research Article

Keywords: Chickpea, Dry root rot, Fusarium wilt, Hyperspectral reflectance, Vegetation indices and early stress detection ·

Posted Date: June 11th, 2026

DOI: https://doi.org/10.21203/rs.3.rs-9871079/v1

Abstract

Early detection of soil-borne fungal diseases is essential for sustaining chickpea (*Cicer arietinum* L.) productivity. This study evaluated hyperspectral canopy reflectance (350–2500 nm) for early detection of dry root rot (DRR; *Macrophomina phaseolina*), Fusarium wilt (*Fusarium oxysporum* f. sp. *ciceri*), and their combined stress under controlled conditions using resistant and susceptible genotypes. Spectral data were collected at regular intervals from 1 to 76 days after sowing (DAS) and used to derive vegetation indices including NDVI, NDWI, PRI, and DSWI. Visual symptoms appeared at 46 DAS (DRR), 42 DAS (wilt), and 43 DAS (combined stress), whereas spectral indices indicated stress-related changes earlier, typically between 36 and 40 DAS. NDVI reflected early reductions in canopy vigor, PRI captured changes in photosynthetic activity, and NDWI and DSWI indicated alterations in plant water status, with DSWI showing comparatively consistent early sensitivity. Resistant genotypes maintained relatively stable NIR reflectance and water-sensitive spectral responses, while susceptible genotypes exhibited reduced NIR reflectance and increased SWIR absorption. Significant differences ($p < 0.001$) were observed for NDVI, PRI, and DSWI between genotype groups. These findings suggest that hyperspectral indices can provide early indications of disease-associated stress in chickpea, with potential applications in phenotyping and crop monitoring.

Introduction

Chickpea (*Cicer arietinum* L.) is an important pulse crop widely cultivated in semi-arid regions and serves as a major source of dietary protein. It contributes significantly to nutritional security and agricultural sustainability due to its high protein content (20–22%) and ability to fix atmospheric nitrogen, thereby improving soil fertility (Jukanti et al. 2012; Gaur et al. 2010). Despite its importance, productivity remains below potential levels, largely due to biotic and abiotic stresses (Kumar and Malik 2022; FAOSTAT 2023; IIPR 2024). This substantial yield gap highlights the need for improved stress management strategies. Among biotic stresses, soil-borne diseases such as dry root rot (DRR) and Fusarium wilt are particularly destructive and pose serious challenges to sustainable chickpea production.

Dry root rot, caused by *Macrophomina phaseolina*, is a major disease in chickpea-growing regions, especially under high temperature and moisture stress conditions (Soni et al. 2022). The pathogen is a necrotrophic fungus with a wide host range (> 500 species) and survives in soil for long periods through microsclerotia (Gupta et al. 2012; Islam et al. 2012). Infected plants exhibit dark, dry, and rotting roots with visible microsclerotia, straw-colored stems, leaf drooping, and eventual plant death (Sharma et al. 2016). Yield losses due to DRR range from 5% under mild infection to 50% under moderate epidemics and may reach up to 80–100% under severe conditions in susceptible genotypes (Ghosh et al. 2013; Pande et al. 2012). Similarly, Fusarium wilt, caused by *Fusarium oxysporum* f. sp. *ciceri*, is another major soil-borne disease of chickpea. The disease is characterized by drooping of leaves, vascular discoloration, and eventual wilting, while roots generally remain intact without microsclerotia (Sharma et al. 2016). The presence of multiple pathogenic races further complicates breeding and management strategies (Jiménez-Fernández et al. 2011). Yield losses due to wilt typically range from 10–15%, but

may reach up to 60% under severe infection (Dubey et al. 2010). Together, DRR and Fusarium wilt significantly reduce chickpea yield and seed quality, making them major constraints to stable production.

Field spectroscopy enables monitoring of crop health by capturing variations in canopy spectral reflectance associated with physiological changes. Stress conditions such as disease, drought, or nutrient deficiency alter pigment composition and plant structure, leading to measurable changes in reflectance in visible and infrared regions (Yang et al. 2010; Jacquemoud and Ustin 2001). Unlike conventional biochemical methods, spectral techniques provide rapid and non-destructive assessment of plant status (Gitelson et al. 2006). Several studies have successfully used spectral data at specific wavelengths, spectral ratios, and red-edge regions to assess pigment levels and plant stress responses (Gitelson et al. 2002; Haboudane et al. 2008; Jones and Vaughan 2010).

Conventionally, plant diseases are identified through visual symptom assessment, often after the infection has progressed significantly. This approach is time-consuming, labor-intensive, and frequently ineffective for timely disease management, as control measures such as fungicide application are most effective during early infection stages. Biological and molecular diagnostic methods, although accurate, are expensive, time-consuming, and limited in scalability for large-area monitoring (Ristaino et al. 2021; Villamor et al. 2019). In chickpea, disease diagnosis largely relies on symptom observation and laboratory assays, which are often too late for effective intervention and unsuitable for high-throughput screening (Sankaran et al. 2010). These limitations highlight the need for rapid, reliable, and non-destructive methods for early disease detection.

In this context, hyperspectral imaging (HSI) has emerged as a promising tool for early plant disease detection (Singh et al. 2020). Hyperspectral imaging exploits plant interactions with different regions of the electromagnetic spectrum to capture detailed information on biochemical composition and structural characteristics (Mahlein et al. 2012). Unlike conventional RGB imaging, HSI includes near-infrared information, enabling detection of subtle physiological changes before visible symptoms appear (Rumpf et al. 2010). By combining imaging and spectroscopy, hyperspectral systems acquire reflectance data across hundreds of narrow, contiguous spectral bands spanning the visible (VIS), near-infrared (NIR), and short-wave infrared (SWIR) regions. Each pixel thus contains a complete spectral signature, allowing detection of subtle biochemical and physiological changes in plants (Lu and Rasmussen 2012). In chickpea, infections such as dry root rot and Fusarium wilt induce physiological alterations including stomatal closure, reduced transpiration, decreased photosynthetic activity, chlorophyll degradation, tissue water loss, and canopy thinning. These changes significantly modify spectral reflectance, particularly in the VIS and NIR regions, enabling disease detection well before the appearance of visible symptoms (Mahlein 2016).

Hyperspectral imaging has demonstrated strong potential in agriculture for detecting plant diseases such as rust and powdery mildew in wheat (Bauriegel and Herppich 2014), viral infections in tomato (Xie et al. 2017), and various abiotic stresses including nutrient deficiency and drought (Behmann et al. 2015). However, its application in pulse crops, particularly chickpea, remains limited. Developing

disease-specific spectral markers for dry root rot (DRR) and Fusarium wilt would support high-throughput phenotyping for resistance breeding, enable timely disease surveillance in farmer fields, and contribute to precision disease management for reducing yield losses.

The present study evaluates the potential of hyperspectral reflectance for early detection of DRR and Fusarium wilt in chickpea. By analyzing temporal changes in canopy spectral reflectance between resistant and susceptible genotypes, the study aims to (i) characterize physiological responses of resistant and susceptible genotypes under pathogen stress and (ii) identify early spectral indicators associated with disease onset prior to visible symptom expression. This work provides a foundation for developing rapid, non-destructive tools for disease monitoring in chickpea, with applications in resistance breeding and precision crop management.

Materials and Methods

Experimental setup

The experiment was conducted to evaluate spectral reflectance responses of resistant and susceptible chickpea genotypes to dry root rot (DRR) and Fusarium wilt under controlled pot culture conditions. Genotypes with known differences in resistance were grown in pots and maintained following recommended agronomic practices.

Artificial inoculation was performed using two soil-borne pathogens: *Macrophomina phaseolina* (causing DRR) and *Fusarium oxysporum* f. sp. *ciceri* (causing wilt), following standardized protocols described by Nene and Reddy (1987) and Singh et al. (2014). The experimental treatments consisted of three groups: (i) DRR treatment, including resistant and susceptible genotypes inoculated with *M. phaseolina*; (ii) wilt treatment, including resistant and susceptible genotypes inoculated with *F. oxysporum* f. sp. *ciceri*; and (iii) combined infection treatment, where susceptible genotypes were inoculated with both pathogens.

The experiment was laid out in a completely randomized design (CRD) with two replications per genotype. Each replication consisted of one pot containing three plants to ensure sufficient canopy development for hyperspectral measurements. A total of nine genotypes were included (Electronic Supplementary Table 1). Of these RVSSG 64 and JSC 37 were earlier reported to be resistant, whereas BG 3062, L 550, JG 62, and Vijay were reported to be susceptible (Soni et al. 2026). For wilt, resistant genotypes used were Phule Vishwaraj and WR 315, while susceptible genotypes used were NBeG 1428 and JG 62. The genotype JG 62, known for its high susceptibility to DRR as well as wilt was included across all treatments to evaluate combined disease effects.

The experiment was conducted at the Hyperspectral Imaging Laboratory, Mahatma Phule Krishi Vidyapeeth (MPKV), Rahuri, India (Electronic Supplementary Fig. 1). The region has a semi-arid tropical climate, with temperatures ranging from 28–32°C during the day and 16–20°C at night during the experimental period. All pots were maintained under uniform conditions with consistent irrigation and pest management practices to minimize environmental variability and ensure that observed stress

responses were primarily due to pathogen inoculation. The results are interpreted in terms of comparative stress responses among genotypes.

Spectral data acquisition and vegetation indices

Spectral reflectance of the chickpea canopy was recorded at alternate-day intervals from 1 day after sowing (DAS) to 76 DAS using a field spectroradiometer (HR-1024i, SVC, USA). The instrument measures reflectance across the 350–2500 nm range with 1 nm spectral resolution, covering the ultraviolet (UV, 350–400 nm), visible (VIS, 400–700 nm), near-infrared (NIR, 700–1300 nm), and short-wave infrared (SWIR, 1300–2500 nm) regions. Prior to each measurement, the instrument was calibrated using a standard white reference panel, and data acquisition followed established protocols. Observations were conducted between 10:00 and 14:00 h under stable illumination conditions to minimize diurnal variability. The sensor was positioned at nadir (90°) at an approximate height of 1 m above the canopy. Spectral data processing and resampling were performed using the proprietary SVC software provided with the instrument.

From the spectral data, four vegetation indices were computed to assess plant physiological status and stress responses: Normalized Difference Vegetation Index (NDVI), Normalized Difference Water Index (NDWI), Photochemical Reflectance Index (PRI), and Disease Sensitive Water Index (DSWI). NDVI was used to estimate canopy vigor and chlorophyll content (Rouse et al. 1973), whereas NDWI provided information on plant water status and moisture dynamics (Gao 1996). PRI was used to monitor variations in photosynthetic efficiency through changes in the xanthophyll cycle (Gamon et al. 1992). DSWI, calculated using absorption features in the NIR–SWIR transition region, has been reported to be sensitive to disease-induced water imbalance and biotic stress (Mahlein et al. 2012; Stuckens et al. 2011). The formulations and spectral characteristics of these indices are summarized in Table 1.

Table 1
Summary of vegetation indices studied in the present investigation

Index	Formula	Wavelengths Used (nm)	Interpretation	Reference
NDVI	$\mathrm{NDVI} = \frac{R_{860} - R_{680}}{R_{860} + R_{680}}$	860 (NIR), 680 (Red)	Sensitive to chlorophyll content and vegetation health	Rouse et al. 1973
NDWI	$\mathrm{NDWI} = \frac{R_{860} - R_{1240}}{R_{860} + R_{1240}}$	860 (NIR), 1240 (SWIR)	Indicates plant water stress and canopy water content	Gao, 1996
PRI	$\mathrm{PRI} = \frac{R_{531} - R_{570}}{R_{531} + R_{570}}$	531, 570 (VIS)	Reflects photosynthetic activity and xanthophyll cycle	Gamon et al. 1992
DSWI	$\mathrm{DSWI} = \frac{R_{970} - R_{1200}}{R_{970} + R_{1200}}$	970 (NIR), 1200 (SWIR)	Highly responsive to disease-induced water imbalance	Mahlein et al. 2012 & Stuckens et al. 2011

For spectral signature analysis, resistant genotypes were considered as relatively less affected reference groups, whereas susceptible genotypes represented higher disease response conditions. The genotype JG 62, known for its high susceptibility to both DRR and wilt, was additionally included to evaluate combined infection effects. Representative spectral signatures were generated by averaging reflectance values within resistant and susceptible groups. Comparative analysis was performed across the full spectral range (350–2500 nm), encompassing the VIS, NIR, and SWIR regions.

Data analysis

Spectral observations were collected at alternate-day intervals throughout the crop growth period, and the raw data were processed using the SVC software package (SVC Inc., 2019). For each genotype, spectral reflectance values were averaged across replications to reduce measurement variability. Subsequently, group-level means were computed by averaging resistant and susceptible genotypes separately. These mean reflectance values were used to calculate vegetation indices, including NDVI, NDWI, PRI, and DSWI.

Since spectral measurements were acquired on alternate days, the resulting index values were interpolated using a linear interpolation approach to generate continuous daily datasets spanning 1–76 DAS. This interpolation facilitated the analysis of temporal trends and enabled consistent comparison of index trajectories across genotypes and treatments.

Statistical analyses were performed to evaluate differences between resistant and susceptible groups. Independent sample t-tests were used to assess differences in index values, while Pearson correlation analysis was conducted to examine relationships among vegetation indices. Temporal dynamics of vegetation indices were visualized using line plots generated in Python and Microsoft Excel.

For disease phenotyping, early detection was defined as the earliest observable and consistent divergence in vegetation index trajectories between resistant and susceptible groups occurring prior to the appearance of visible symptoms. This criterion enabled estimation of the lead time by which hyperspectral sensing could detect disease onset relative to conventional visual assessment.

Results

Continuous spectral observations were used to derive vegetation indices, which were interpolated to generate daily values from 1 to 76 DAS. These indices were analyzed separately for resistant and susceptible genotypes under DRR, wilt, and combined DRR–wilt conditions to evaluate their potential for early disease detection. Visual symptoms of DRR were observed at 46 DAS, wilt at 42 DAS, and combined infection (JG 62) at 43 DAS.

Diagnosis of dry root rot

Vegetation indices clearly differentiated resistant and susceptible genotypes under DRR conditions and showed detectable changes prior to the appearance of visible symptoms (Fig. 1A–D). NDVI increased steadily during the early vegetative phase (10–30 DAS) in both groups (Fig. 1A). Resistant genotypes exhibited a temporary dip around 20 DAS followed by recovery after 30 DAS, whereas susceptible genotypes showed a continuous increase without recovery. After 40 DAS, NDVI declined in susceptible genotypes, approximately 6 days before the onset of visible symptoms (46 DAS), while resistant genotypes maintained relatively stable values.

NDWI values remained comparable between groups up to 30 DAS (Fig. 1B). From 40 DAS onward, resistant genotypes maintained higher and stable values, whereas susceptible genotypes showed a decline.

PRI remained near baseline until approximately 40 DAS (Fig. 1C). Around symptom onset (46 DAS), resistant genotypes exhibited a transient increase followed by partial recovery, while susceptible genotypes showed a continuous decline after 40 DAS.

DSWI in susceptible genotypes increased during 30–40 DAS and showed a marked change around 40 DAS, preceding visible symptom expression by nearly one week (Fig. 1D). In contrast, resistant genotypes exhibited relatively stable DSWI values throughout the observation period.

Statistical analyses supported these observations. Significant differences between resistant and susceptible genotypes were observed for NDVI, PRI, and DSWI ($p < 0.001$), while NDWI showed lower significance ($p = 0.021$) (Electronic Supplementary Table 2). Correlation analysis further indicated strong relationships among indices (Electronic Supplementary Table 3). In resistant genotypes, NDVI showed strong correlations with NDWI ($r = 0.905$, $p < 0.01$) and DSWI ($r = 0.861$, $p < 0.01$), and a moderate correlation with PRI ($r = 0.663$, $p < 0.05$). NDWI and DSWI were highly correlated ($r = 0.987$, $p < 0.01$).

In susceptible genotypes, correlations were generally weaker and less consistent. NDVI showed a moderate correlation with NDWI ($r = 0.610$, $p < 0.05$) and a strong correlation with DSWI ($r = 0.904$, $p < 0.01$). PRI was strongly correlated with NDVI ($r = 0.827$, $p < 0.01$) but showed weaker associations with NDWI and DSWI.

Diagnosis of Fusarium wilt

Hyperspectral vegetation indices (NDVI, NDWI, PRI, and DSWI) showed measurable changes in canopy response prior to the appearance of visible wilt symptoms at 42 DAS (Fig. 2A–D). NDVI increased in both resistant and susceptible genotypes during the early vegetative phase (up to 30 DAS) (Fig. 2A). From 36 DAS onward, NDVI declined in susceptible genotypes, whereas resistant genotypes maintained relatively higher values until after 40 DAS.

NDWI remained stable in both groups up to 30 DAS (Fig. 2B). After 40 DAS, susceptible genotypes exhibited a gradual decline with fluctuations, while resistant genotypes maintained comparatively stable values.

PRI remained near baseline until approximately 40 DAS (Fig. 2C). At symptom onset (42 DAS), susceptible genotypes showed a sharp decline, whereas resistant genotypes exhibited a transient increase followed by stabilization.

DSWI increased gradually in both groups until 30 DAS (Fig. 2D). From 40 DAS onward, susceptible genotypes showed a decline, whereas resistant genotypes remained stable or slightly positive.

Statistical analyses supported these observations. Significant differences between resistant and susceptible genotypes were observed for NDVI and PRI ($p < 0.001$), whereas NDWI ($p = 0.117$) and DSWI ($p = 0.078$) were not statistically significant (Electronic Supplementary Table 4). Correlation analysis further revealed relationships among vegetation indices (Electronic Supplementary Table 5).

In resistant genotypes, NDVI showed strong correlation with NDWI ($r = 0.841$, $p < 0.01$) and moderate correlation with DSWI ($r = 0.751$, $p < 0.05$). PRI was positively correlated with NDVI ($r = 0.774$, $p < 0.05$) and NDWI ($r = 0.640$). The strongest association was observed between NDWI and DSWI ($r = 0.979$, $p < 0.01$).

In susceptible genotypes, NDVI showed moderate correlation with NDWI ($r = 0.545$) and PRI ($r = 0.811$, $p < 0.05$), but weaker association with DSWI ($r = 0.415$). PRI exhibited moderate correlations with NDWI ($r = 0.596$) and DSWI ($r = 0.496$), while the strongest correlation was observed between NDWI and DSWI ($r = 0.950$, $p < 0.01$).

Diagnosis of combined (DRR and wilt) stress

In the susceptible genotype JG 62, visual symptoms of combined DRR and wilt appeared at 43 DAS (Fig. 3A–D). NDVI increased steadily until 30 DAS, followed by a sharp decline around 40 DAS, preceding the appearance of visible symptoms (Fig. 3A). NDWI also showed a reduction at approximately 40 DAS (Fig. 3B).

PRI exhibited a marked decline at 40 DAS (Fig. 3C). DSWI increased until approximately 35 DAS and then declined sharply after 40 DAS (Fig. 3D).

As only a single susceptible genotype was evaluated under combined stress, group-wise t-tests were not performed. Correlation analysis indicated relationships among vegetation indices (Electronic Supplementary Table 6). NDVI showed a strong correlation with PRI ($r = 0.884$, $p < 0.01$) and a moderate correlation with DSWI ($r = 0.666$, $p < 0.05$). PRI was strongly correlated with DSWI ($r = 0.862$, $p < 0.01$) and moderately with NDWI ($r = 0.602$, $p < 0.05$). NDWI also showed a significant correlation with DSWI ($r = 0.722$, $p < 0.05$), whereas the correlation between NDVI and NDWI was weaker ($r = 0.577$).

A comparison of visual observations and hyperspectral indices showed that index-based changes occurred prior to the appearance of visible symptoms (Table 2). For DRR, visual symptoms were observed at 46 DAS, whereas changes in NDVI, NDWI, PRI, and DSWI were detected at approximately 40 DAS. In wilt, visual symptoms appeared at 42 DAS, while NDVI and DSWI showed changes at 36 DAS,

and NDWI and PRI at 40–42 DAS. For combined DRR–wilt infection, symptoms were observed at 43 DAS, whereas all indices showed changes around 40 DAS.

Table 2
Comparative summary of visual and hyperspectral observations in chickpea disease diagnosis days after sowing

Disease/indices	Dry root rot	Wilt	Dry root rot and Wilt combined
Onset of visual symptoms	46	42	43
NDVI	40	36	40
NDWI	40	40	43
PRI	40	36	40
DSWI	40	40	40

Electronic Supplementary Fig. 1. Experimental setup for hyperspectral data collection in chickpea. **A.** Chickpea genotypes grown in pots for disease evaluation. **B and C.** Hyperspectral sensing system using the SVC HR-1024i spectroradiometer with controlled illumination for canopy spectral reflectance measurements under pot culture conditions

Spectral signatures under stress

Spectral signatures of resistant and susceptible chickpea genotypes showed clear differences under disease conditions (Fig. 4A–C). Under DRR stress, resistant genotypes exhibited higher reflectance in the NIR region (700–1300 nm), whereas susceptible genotypes showed comparatively lower reflectance and increased absorption in the red-edge region (~ 680 nm) (Fig. 4A).

Under wilt conditions, resistant genotypes maintained higher reflectance across both NIR and SWIR regions compared to susceptible genotypes (Fig. 4B). Susceptible genotypes showed reduced reflectance in the NIR region and increased absorption in the water-sensitive bands (1400–1500 nm and 1900–2000 nm).

In the combined infection (DRR + wilt), the susceptible genotype JG 62 showed a pronounced reduction in NIR reflectance and increased absorption in the SWIR region compared to individual disease conditions (Fig. 4C).

Discussion

Dry root rot

The present study demonstrates that hyperspectral vegetation indices can detect dry root rot (DRR) stress several days prior to the appearance of visible symptoms. Temporal changes in NDVI and PRI indicated early alterations in canopy condition and photosynthetic activity. In resistant genotypes, the

transient dip followed by recovery suggests a regulated physiological response under pathogen stress, whereas susceptible genotypes showed a sustained decline after ~ 40 DAS, indicating progressive stress development.

Water-related indices (NDWI and DSWI) further captured early changes associated with DRR infection. The observed divergence in DSWI prior to symptom appearance aligns with the infection mechanism of *Macrophomina phaseolina*, which causes root necrosis and disrupts water uptake and transport (Pande et al. 2012; Sharma et al. 2010). The early response of DSWI highlights the sensitivity of SWIR-based indices in detecting disease-induced water imbalance before visible wilting occurs. These findings are consistent with previous studies reporting that hyperspectral indices sensitive to pigment and water dynamics provide early detection of plant diseases (Mahlein 2016). Similarly, Stuckens et al. (2011) demonstrated that SWIR-based indices are effective in distinguishing healthy and infected vegetation. The observed recovery pattern in resistant genotypes supports earlier reports on genotype-specific defence responses limiting DRR progression (Singh et al. 2014).

Overall, resistant genotypes maintained more stable and coordinated spectral responses, whereas susceptible genotypes exhibited greater variability and decline in index values. Among the evaluated indices, NDVI, PRI, and DSWI showed consistent sensitivity to DRR stress, indicating their suitability as non-destructive indicators for early disease detection in chickpea. However, the results should be interpreted in a relative context due to the controlled experimental conditions and limited replication.

Wilt diagnosis

Fusarium wilt, caused by *Fusarium oxysporum* f. sp. *ciceri*, typically occurs during the early reproductive stage (35–45 DAS), when the pathogen invades xylem vessels, restricting water and nutrient transport and leading to wilting, chlorosis, and necrosis (Haware and Nene 1980; Pande et al. 2010). The hyperspectral responses observed in this study were consistent with this disease progression. Temporal changes in NDVI indicated early reductions in canopy vigor and chlorophyll content, with detectable deviations occurring approximately six days prior to visible symptom expression.

PRI also showed sensitivity to wilt stress, with susceptible genotypes exhibiting a decline around symptom onset, while resistant genotypes showed a transient increase followed by stabilization. These responses suggest differences in physiological regulation between resistant and susceptible genotypes under pathogen stress. Similar observations have been reported by Mahlein (2016), who highlighted the effectiveness of pigment- and photosynthesis-related indices, such as NDVI and PRI, in detecting vascular diseases.

In contrast, water-related indices (NDWI and DSWI) showed comparatively weaker and less consistent responses, likely reflecting the indirect effect of vascular blockage on canopy water status during early stages of infection. Overall, NDVI and PRI emerged as more sensitive indicators of wilt stress, with resistant genotypes maintaining more stable spectral responses, whereas susceptible genotypes

exhibited greater variability under infection conditions. As with DRR, these findings should be interpreted as relative trends under controlled experimental conditions.

Diagnosis of combined stress of DRR and wilt

The DRR–wilt complex represents a highly destructive condition in chickpea, where two distinct pathogenic mechanisms operate simultaneously. Macrophomina phaseolina induces root necrosis and restricts water uptake, while Fusarium oxysporum f. sp. ciceri obstructs xylem vessels and disrupts vascular transport (Nene and Reddy 1987; Pande et al. 2012). The combined effect accelerates canopy senescence, enhances chlorophyll degradation, and induces severe water stress. These physiological disruptions are reflected in the simultaneous changes observed across all vegetation indices (NDVI, NDWI, PRI, and DSWI) around 40 DAS, preceding visible symptom expression.

The sensitivity of hyperspectral indices to combined stress conditions highlights their potential for monitoring multi-pathogen interactions. Both pigment-related indices (NDVI and PRI) and water-sensitive indices (NDWI and DSWI) responded to the dual infection, indicating that multiple physiological pathways are affected concurrently. This observation is consistent with Mahlein (2016), who emphasized that integrating pigment- and water-sensitive indices improves detection of complex plant stresses. Similarly, Stuckens et al. (2011) demonstrated that SWIR-based indices can capture subtle water-related changes that are not detectable using pigment-based indices alone.

A comparative assessment showed that visual symptoms appeared at 46 DAS (DRR), 42 DAS (wilt), and 43 DAS (combined stress), whereas hyperspectral indices indicated deviations earlier, typically between 36 and 40 DAS. Among the indices, NDVI and DSWI showed relatively earlier and more consistent responses under both individual and combined stress conditions, reflecting chlorophyll degradation and water imbalance, respectively. In contrast, NDWI and PRI exhibited comparatively delayed or variable responses, possibly due to the indirect nature of vascular disruption on canopy water status and photosynthetic adjustments during early infection stages.

These findings are consistent with previous studies reporting that spectral indices associated with canopy vigor and water status are sensitive indicators of biotic stress (Mahlein et al. 2012; Rouse et al. 1973). The ability of hyperspectral indices to detect combined stress prior to visible symptom development underscores their potential for studying multi-pathogen interactions in chickpea. However, these observations are based on controlled experimental conditions and should be interpreted as indicative of relative stress responses rather than direct measures of disease severity.

Spectral signature

The spectral differences observed between resistant and susceptible genotypes indicate that hyperspectral reflectance can capture stress-induced physiological changes in chickpea. Under DRR conditions, susceptible plants showed reduced reflectance in the NIR region and increased absorption in the red-edge region, consistent with chlorophyll degradation and structural damage associated with root necrosis caused by Macrophomina phaseolina (Sharma et al. 2010).

In wilt-affected plants, depression in NIR reflectance along with increased absorption in SWIR regions was observed in susceptible genotypes. These patterns are indicative of disrupted water transport and loss of tissue turgor resulting from vascular blockage caused by Fusarium oxysporum infection (Pande et al. 2012).

Under combined DRR and wilt stress, the susceptible genotype JG 62 exhibited more pronounced reductions in NIR reflectance and stronger absorption in SWIR regions compared to individual disease conditions. This suggests a compounded physiological impact, likely due to simultaneous disruption of root function and vascular transport. Such combined effects may accelerate canopy senescence and contribute to rapid decline in plant health.

Across all stress conditions, resistant genotypes consistently maintained relatively higher NIR reflectance and more stable responses in water-sensitive spectral regions, whereas susceptible genotypes showed clear deviations. These observations are consistent with earlier studies demonstrating that NIR reflectance is associated with canopy structure and vigor, while SWIR regions are sensitive to plant water status (Mahlein et al. 2012; Stuckens et al. 2011; Rouse et al. 1973).

Overall, the NIR and SWIR regions emerged as important spectral domains for distinguishing stress responses in chickpea. While these results highlight the potential of hyperspectral reflectance for early and non-destructive detection of disease-associated stress, further validation under field conditions is required to establish their robustness for large-scale applications.

Conclusions

The present study highlights the potential of hyperspectral sensing as a non-destructive approach for early detection of dry root rot (DRR), Fusarium wilt, and their combined stress in chickpea. Across resistant and susceptible genotypes, vegetation indices (NDVI, NDWI, PRI, and DSWI) exhibited clear temporal divergence, with stress-related changes detected approximately 4–6 days prior to the appearance of visible symptoms. This demonstrates the ability of hyperspectral indices to extend the diagnostic window beyond conventional visual assessment.

Among the indices, NDVI and DSWI showed relatively earlier and more consistent responses, reflecting changes in chlorophyll status and disease-induced water imbalance, respectively. PRI and NDWI provided complementary information related to photosynthetic efficiency and plant water status. These combined responses indicate that hyperspectral indices can capture multiple physiological processes associated with disease development.

Spectral signature analysis further supported these findings. Resistant genotypes maintained higher reflectance in the near-infrared (NIR) region and more stable responses in water-sensitive short-wave infrared (SWIR) bands, whereas susceptible genotypes showed reduced NIR reflectance and increased SWIR absorption. These patterns are consistent with physiological effects of pathogen infection, including chlorophyll degradation, impaired water uptake, and vascular dysfunction. Under combined

DRR and wilt stress, more pronounced spectral changes were observed, indicating compounded effects on canopy structure and water status.

Overall, the integration of vegetation indices and spectral reflectance patterns provides a useful framework for distinguishing relative stress responses among chickpea genotypes under controlled conditions. While the results indicate the potential of hyperspectral sensing for early disease detection and phenotyping, further validation under field conditions is required before large-scale application. It is important to note that the present study was conducted under controlled conditions with limited replication, and no direct pathogen quantification was performed. Therefore, the results represent physiological stress responses associated with disease progression rather than absolute measures of infection severity.

Future research should focus on multi-location field validation, integration with UAV-based hyperspectral platforms, and the development of robust data-driven models for automated stress detection. Such advancements will support the development of scalable digital tools for disease monitoring and management in chickpea and other pulse crops.

Declarations

Acknowledgements

VBT gratefully acknowledge the financial support received from the Chhatrapati Shahu Maharaj Research, Training and Human Development Institute (SARTHI), Government of Maharashtra, India for the doctoral research programme.

Funding statement

During the course of study, funding was provided to authors by the Government of Maharashtra (Grant no. MPV1422/L.No.253/7-A dated 21.03.2023).

Authors' contributions

VBT: Methodology, data collection, formal analysis, writing-original draft.

VSM: Statistical analysis, visualization, writing-original draft.

SAK: Conceptualization, resources, methodology, review and editing.

PLK: Conceptualization, designed experiment, supervision, validation, writing—review and editing.

Conflict of interest

All authors declare no conflict of interest.

Ethical approval

This article does not contain any studies involving human participants or animals.

Consent to publish

All authors agree to publish.

Data availability

The datasets generated during the current study are available from the corresponding author on reasonable request.

References

1. Ariana DP, Lu R, Guyer DE (2006) Near-infrared hyperspectral reflectance imaging for detection of bruises on pickling cucumbers. Comput Electron Agric 53:60–70. https://doi.org/10.1016/j.compag.2006.04.001
2. Bauriegel E, Herppich WB (2014) Hyperspectral and chlorophyll fluorescence imaging for early detection of plant diseases, with special reference to Fusarium infections on wheat. Agriculture 4(1):32–57. https://doi.org/10.3390/agriculture4010032
3. Behmann J, Mahlein AK, Rumpf T, Römer C, Plümer L (2015) A review of advanced machine learning methods for the detection of biotic stress in precision crop protection. Precision Agric 16:239–260. https://doi.org/10.1007/s11119-014-9372-7
4. Dubey SC, Singh SR, Singh B (2010) Morphological and pathogenic variability of Indian isolates of Fusarium oxysporum f. sp. ciceris causing chickpea wilt. Arch Phytopathol Plant Prot 43:174–189. https://doi.org/10.1080/03235400802021108
5. FAOSTAT (2023) Chickpea production statistics. Food and Agriculture Organization of the United Nations. https://www.fao.org/faostat
6. Gamon JA, Peñuelas J, Field CB (1992) A narrow-waveband spectral index that tracks diurnal changes in photosynthetic efficiency. Remote Sens Environ 41:35–44. https://doi.org/10.1016/0034-4257(92)90059-S
7. Gao B (1996) NDWI: A normalized difference water index for remote sensing of vegetation liquid water from space. Remote Sens Environ 58:257–266. https://doi.org/10.1016/S0034-4257(96)00067-3
8. Gaur PM, Tripathi S, Gowda CLL, Ranga Rao GV, Sharma HC, Pande S, Sharma M (2010) Chickpea Seed Production Manual. ICRISAT, Patancheru, India
9. Ghosh R, Sharma M, Telangre R, Pande S (2013) Occurrence and distribution of chickpea diseases in central and southern parts of India. Am J Plant Sci 4:940–944. https://doi.org/10.4236/ajps.2013.44116
10. Gitelson A, Kaufman Y, Stark R, Rundquist D (2002) Novel algorithms for remote estimation of vegetation fraction. Remote Sens Environ 80:76–87. https://doi.org/10.1016/S0034-

4257(01)00289-9

11. Gitelson A, Keydan G, Merzlyak MN (2006) Three-band model for noninvasive estimation of chlorophyll, carotenoids, and anthocyanin contents in higher plant leaves. Geophys Res Lett 33:L11402. https://doi.org/10.1029/2006GL026457
12. Gupta GK, Sharma SK, Ramteke R (2012) Biology, epidemiology and management of Macrophomina phaseolina (Tassi) Goid with special reference to charcoal rot of soybean. J Phytopathol 160:167–180. https://doi.org/10.1111/j.1439-0434.2012.01884.x
13. Haboudane D, Tremblay N, Miller JR, Vigneault P (2008) Remote estimation of crop chlorophyll content using spectral indices derived from hyperspectral data. IEEE Trans Geosci Remote Sens 46:423–437. https://doi.org/10.1109/TGRS.2007.904836
14. Haware MP, Nene YL (1980) Influence of wilt at different stages on yield loss in chickpea. Trop Grain Legume Bull 19:38–40
15. IIPR (2024) Annual Report. Indian Institute of Pulses Research, ICAR, Kanpur, India
16. Islam MS, Haque MS, Islam MM, Emdad EM, Halim A, Hossen QMM et al (2012) Tools to kill: genome of one of the most destructive plant pathogenic fungi Macrophomina phaseolina. BMC Genomics 13:493. https://doi.org/10.1186/1471-2164-13-493
17. Jacquemoud S, Ustin SL (2001) Leaf optical properties: a state of the art. In: Proceedings of the 8th International Symposium on Physical Measurements and Signatures in Remote Sensing. CNES, France, pp 223–232
18. Jiménez-Fernández D, Montes-Borrego M, Jiménez-Díaz RM, Navas-Cortés JA, Landa BB (2011) In planta and soil quantification of Fusarium oxysporum f. sp. ciceris and evaluation of Fusarium wilt resistance in chickpea with a newly developed qPCR assay. Phytopathology 101:250–262. https://doi.org/10.1094/PHYTO-07-10-0190
19. Jones HG, Vaughan RA (2010) Remote sensing of vegetation. Oxford University Press, Oxford
20. Jukanti AK, Gaur PM, Gowda CLL, Chibbar RN (2012) Nutritional quality and health benefits of chickpea (Cicer arietinum L.): a review. Br J Nutr 108(S1):S11–S26. https://doi.org/10.1017/S0007114512000797
21. Kumar V, Malik DP (2022) Trends and economic analysis of chickpea (Cicer arietinum L.) production in India. Legume Res 41(2):739–745. https://doi.org/10.18805/LR-4421
22. Lu G, Rasmussen CR (2012) Hyperspectral image analysis for plant disease detection. Plant Pathol 61:150–164. https://doi.org/10.1111/j.1365-3059.2011.02583.x
23. Mahlein AK (2016) Plant disease detection by imaging sensors — parallels and specific demands for precision agriculture. Comput Electron Agric 138:200–209. https://doi.org/10.1016/j.compag.2017.01.034
24. Mahlein AK, Steiner U, Hillnhütter C, Dehne HW, Oerke EC (2012) Hyperspectral imaging for small-scale analysis of symptoms caused by different sugar beet diseases. Plant Methods 8:3. https://doi.org/10.1186/1746-4811-8-3

25. Nene YL, Reddy MV (1987) Diseases of chickpea and their control. In: Saxena MC, Singh KB (eds) The Chickpea. CAB International, Wallingford, UK, pp 233–270
26. Pande S, Sharma M, Avuthu N, Telangre R (2012) High throughput phenotyping of chickpea diseases: stepwise identification of host plant resistance. Technical Report No. 92. ICRISAT, Patancheru, India
27. Pande S, Sharma M, Gaur PM (2010) Host plant resistance to dry root rot in chickpea. Indian Phytopathol 63:186–188
28. Pande S, Sharma M, Gaur PM (2012) Biology, ecology and management of Fusarium wilt of chickpea. Crop Protect 30(5):464–471. https://doi.org/10.1016/j.cropro.2012.12.017
29. Ristaino JB, Anderson PK, Bebber DP, Brauman KA, Wei Q (2021) The persistent threat of emerging plant disease pandemics to global food security. Proc Natl Acad Sci USA 118:e2022239118. https://doi.org/10.1073/pnas.2022239118
30. Rouse JW, Haas RH, Schell JA, Deering DW (1973) Monitoring vegetation systems in the Great Plains with ERTS. NASA Special Publication 351:309–317
31. Rumpf T, Mahlein AK, Steiner U, Oerke EC, Dehne HW, Plümer L (2010) Early detection and classification of plant diseases with support vector machines based on hyperspectral reflectance. Comput Electron Agric 74:91–99
32. Sankaran S, Mishra A, Ehsani R, Davis C (2010) A review of advanced techniques for detecting plant diseases. Comput Electron Agric 72:1–13. https://doi.org/10.1016/j.compag.2010.02.007
33. Sharma M, Ghosh R, Pande S (2016) Dry root rot (Rhizoctonia bataticola (Taub.) Butler): an emerging disease of chickpea – where do we stand? Arch Phytopathol Plant Protect 48:797–812. https://doi.org/10.1080/03235408.2016.1140564
34. Singh G, Chaudhary RG, Saxena MC (2014) Screening techniques and resistance sources for major chickpea diseases. Legume Res 37:307–315. https://doi.org/10.5958/j.0976-0571.37.4.013
35. Singh V, Sharma N, Singh S (2020) A review of imaging techniques for plant disease detection. Artif Intell Agric 4:229–242. https://doi.org/10.1016/j.aiia.2020.10.002
36. Soni N, Raghuwanshi KS, Kulwal PL (2022) Effect of abiotic factors on the incidence of dry root rot in chickpea (Cicer arietinum L). J Agril Res Tech 47:205–211. https://doi.org/10.56228/JART.2022.47216
37. Soni N, Raghuwanshi KS, Kulwal PL (2026) Identification of sources of resistance to dry root rot in chickpea (*Cicer arietinum* L). Arch Phytopathol Plant Prot (accepted
38. Stuckens J, Verstraeten WW, Delalieux S, Swennen R, Coppin P (2011) A review of remote sensing approaches for vegetation stress detection. Remote Sens Environ 115:297–306. https://doi.org/10.1016/j.rse.2011.05.019
39. SVC (2019) Field Spectroscopy Guide with SVC i-series Spectroradiometers. Spectra Vista Corporation. https://spectravista.com/fieldguidethnx/

40. Varshney RK, Song C, Saxena RK, Azam S, Yu S, Sharpe AG, Cannon S et al (2013) Draft genome sequence of chickpea (Cicer arietinum) provides a resource for trait improvement. Nat Biotechnol 31:240–246. https://doi.org/10.1038/nbt.2491
41. Villamor DEV, Ho T, Rwahnih MA, Martin RR, Tzanetakis I (2019) High throughput sequencing for plant virus detection and discovery. Phytopathology 109:716–725. https://doi.org/10.1094/PHYTO-07-18-0257-RVW
42. Xie C, Yang C, He Y (2017) Hyperspectral imaging for classification of healthy and gray mold diseased tomato leaves with different infection severities. Comput Electron Agric 135:154–162. https://doi.org/10.1016/j.compag.2016.12.015
43. Yang F, Li J, Gan X, Qian Y, Wu X, Yang Q (2010) Assessing nutritional status of Festuca arundinacea by monitoring photosynthetic pigments from hyperspectral data. Comput Electron Agric 70:52–59. https://doi.org/10.1016/j.compag.2009.09.005
44. Zhai Y, Cui L, Zhou X, Gao Y, Fei T, Gao W (2013) Estimation of nitrogen, phosphorus, and potassium contents in the leaves of different plants using laboratory-based visible and near-infrared reflectance spectroscopy: comparison of PLSR and SVM regression methods. Int J Remote Sens 34:2502–2518. https://doi.org/10.1080/01431161.2012.746484

Figures

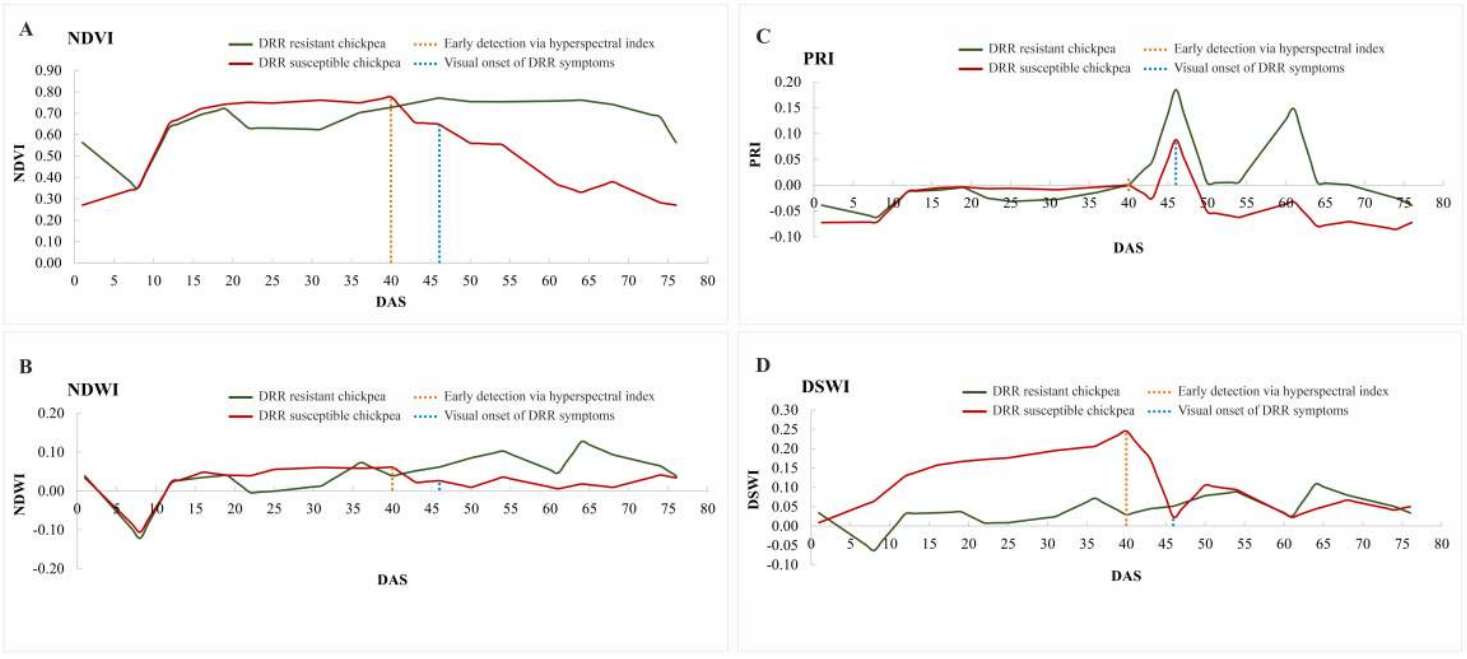

Figure 1

Temporal dynamics of vegetation indices in resistant and susceptible chickpea genotypes subjected to dry root rot (DRR) NDVI NDWI PRI DSWI

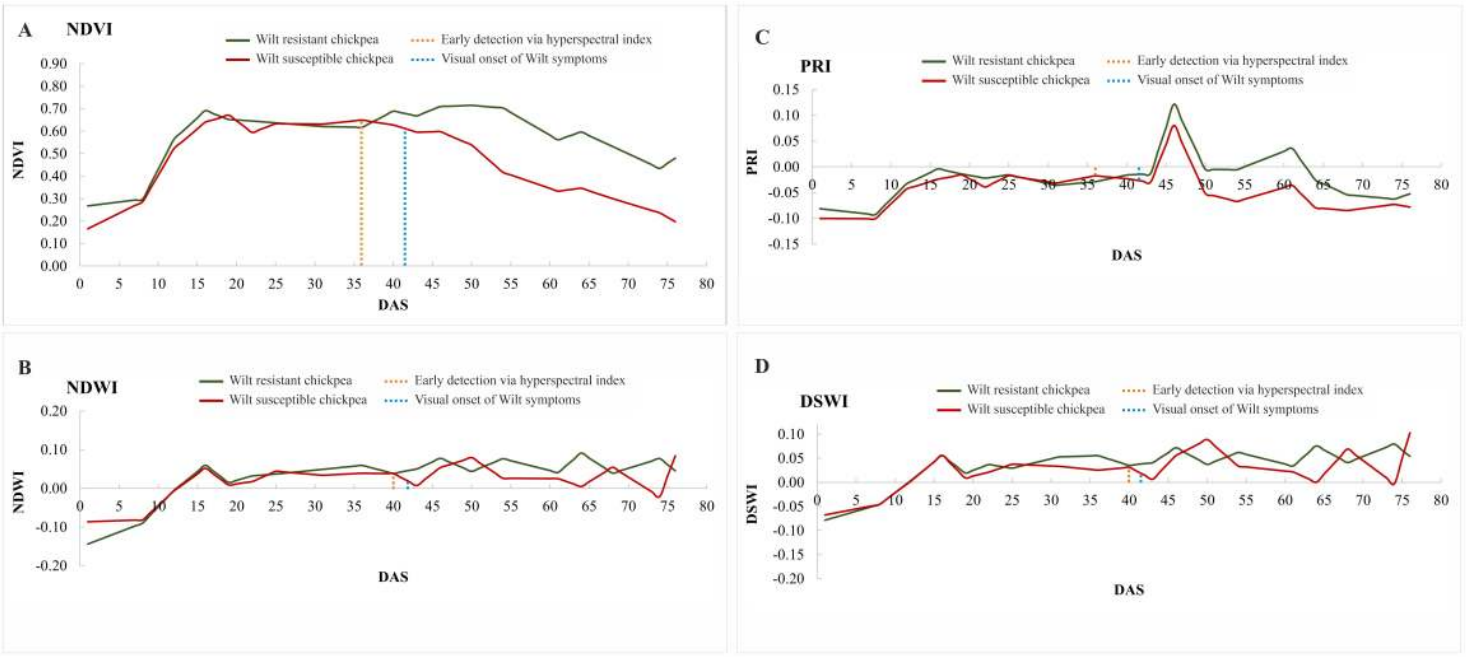

Figure 2

Temporal dynamics of vegetation indices in resistant and susceptible chickpea genotypes subjected to wilt NDVI NDWI PRI DSWI

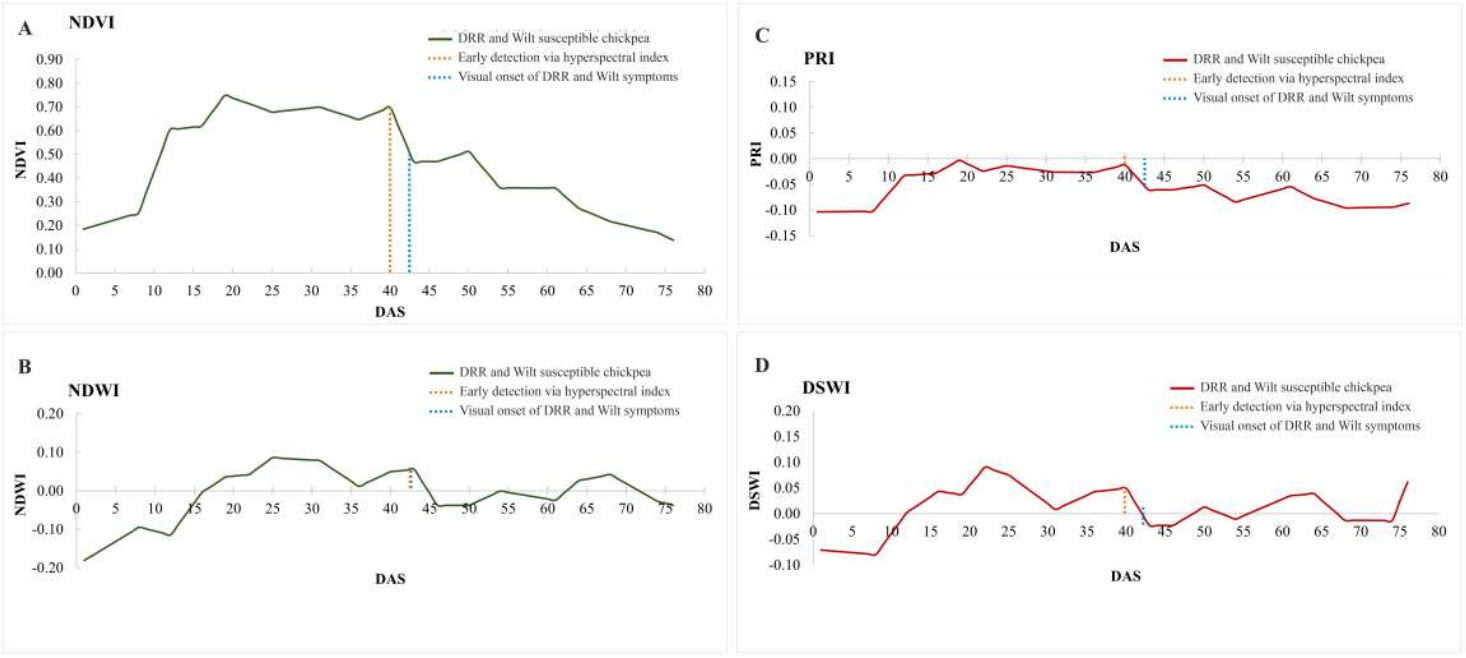

Figure 3

Temporal dynamics of vegetation indices in combined DRR and wilt susceptible chickpea genotype JG 62 NDVI NDWI PRI DSWI

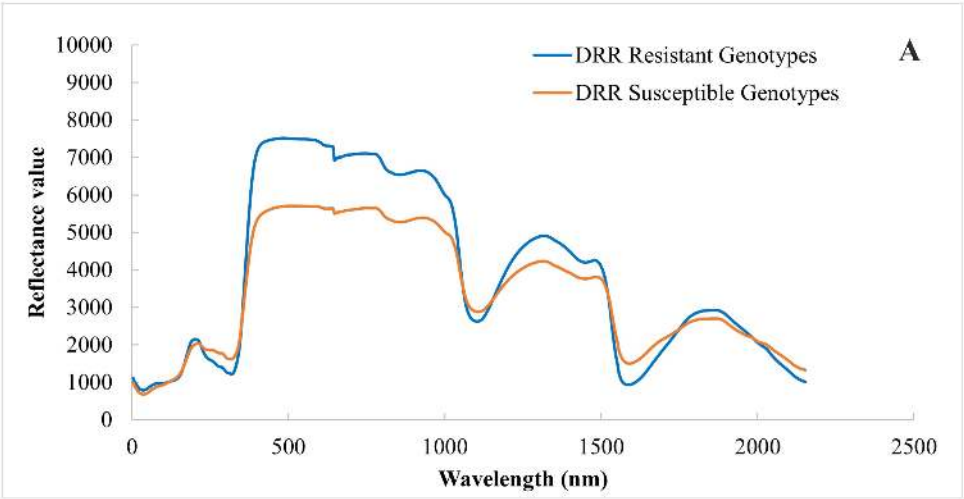

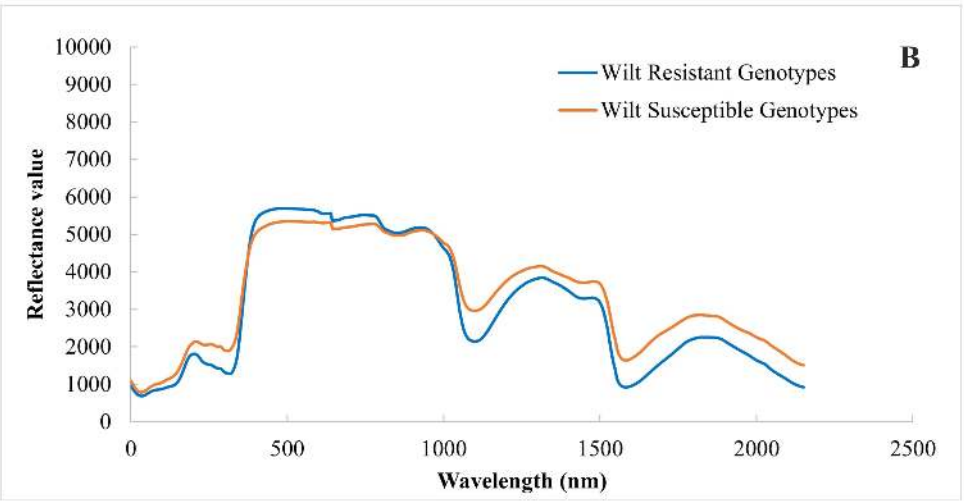

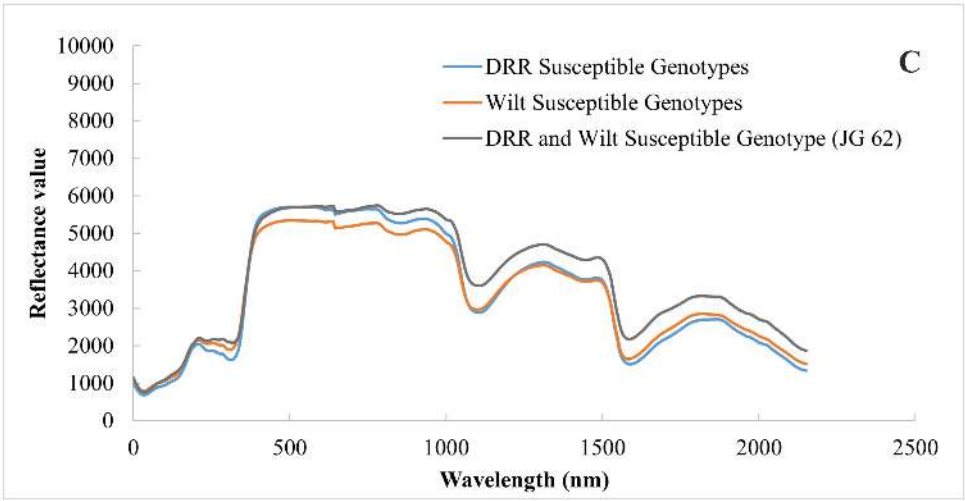

Figure 4

Spectral signatures of disease resistant and susceptible chickpea genotypes DRR Wilt combination of DRR and Wilt

Supplementary Files

This is a list of supplementary files associated with this preprint. Click to download.

- ElectronicSupplementaryFig.1.jpg